Dynamics of inextensible semiflexible filaments

Tanniemola B. Liverpool*
Department of Applied Mathematics, University of Leeds, Woodhouse Lane, Leeds LS2 9JT, United Kingdom and Max-Planck-Institut für Physik Komplexer Systeme, Nöthnitzerstr. 38, D-01187, Dresden, Germany
(Received 13 May 2003; revised manuscript received 18 January 2005; published 15 August 2005)

We address the problem of the fluctuating dynamics of an isolated inextensible and semiflexible filament of length L. By focusing explicitly on two key properties of the filaments—their connectivity and inextensibility—we obtain insights into their dynamics. We calculate the dynamics, and we calculate the correlation functions for chains of finite length taking into account the boundary conditions at the chain ends. We obtain closed-form expressions that separate the internal bending modes from the global rotation modes.

DOI: 10.1103/PhysRevE.72.021805 PACS number(s): 82.35.−x, 87.16.−b, 47.54.+r, 05.65.+b

I. INTRODUCTION

The dynamics of polymeric fluids is important for many processes in biology, chemistry, and physics [1]. Because of the strength of covalent bonds in organic compounds, the dynamics of polymers in a viscous fluids can be accurately described as the dynamics of nearly inextensible chains. At a coarse-grained level, a polymer can be considered to be a chain of *links* whose length fluctuates about some typical size. We emphasize that the links are coarse-grained entities which exist on much longer length scales than the chemical bonds which microscopically hold the chain together.

Since typical *mechanical* experiments on polymeric fluids probe the dynamics of chain configurations rather than the high-frequency dynamics of the link length fluctuations, it is natural to simplify the problem by ignoring the rapid motions of the link length fluctuations and to focus on the dynamics of the more interesting slower modes associated with changes in chain conformations. If, for example, in a simulation the length of the links is held constant by very stiff springs, rapid oscillations occur which dominate and obscure the dynamics of the more important slower modes. Therefore an absolutely inextensible chain is often proposed as a good model for the study of polymer dynamics [1–3]. In spite of this simplification, the dynamics of inextensible chains remains intractable because it entails the study of the constrained Brownian motion of an extended object.

While flexible industrial polymers like polystyrene sulphonate or polyethylene are described by the *freely jointed chain* which consists of $N \gg 1$ links of fixed length ℓ, semiflexible biopolymers like DNA or F-actin are well captured by the Kratky-Porod [4] wormlike chain (WLC) model where chain conformation is described by an an inextensible and differentiable curve. In general for such semiflexible filaments the bending modulus is much smaller than the extensional modulus and the chains are effectively inextensible on the lengths and time scales for which the rigidity of the chain is relevant.

Previous work describing the dynamics of inextensible filaments [5–11] imposes inextensibility by a holonomic constraint. Filament dynamics is described by the *time-varying* position of the center line $\mathbf{r}(s,t)$ (see Fig. 2) whose dynamics is controlled by the balance of viscous, elastic, thermal, and constraint forces. The thermal, viscous, and elastic forces can be expressed in terms of the *unconstrained* position of this line but the inextensibility constraint reduces the phase space of allowed values of $\hat{\mathbf{u}}(s,t) \equiv \partial_s \mathbf{r}$ [12]. Including thermal fluctuations in the motion of the filaments correctly turns out to be rather subtle [2,3,12]. The nonlinear nature of the problem has restricted analytic progress to certain asymptotic limits: namely, a *small amplitude expansion* [13] about a stationary rodlike state. Much progress has been made in those limits but many open questions remain [5,14–16] and the dynamics of inextensible semiflexible filaments continues to be of interest for a variety of problems in material science and biology [17–24].

In this paper, we propose a radically different procedure for describing the dynamics of semiflexible filaments. First we note that the filaments we consider are characterized by two properties. They are (1) inextensible and (2) connected. While, previously, explicitly connected models were studied on which inextensibility was imposed, we propose an explicitly *inextensible* chain on which connectivity is *imposed*. As we will see, this leads to simpler constraints *and* dynamical equations but requires an additional equation. While we focus on using the approach to make analytic calculations of semiflexible filaments in this paper, we expect it to be particularly useful for doing simulations of inextensible polymers. Simulations using our approach would be similar to but have a simpler implementation than needle or rod models used in Brownian dynamics simulations of polymers [25,26].

The outline of the paper is as follows: In the next section II, we introduce the new formalism and compare it to previous approaches. In Sec. III we develop the calculational methods used to evaluate the dynamical properties of the chain. There we consider the fluctuating dynamics of chains shorter than a persistence length and perform a small-amplitude expansion around a rod whose axis is free to rotate. We emphasise that this is *not* a systematic expansion in a small parameter but rather a restriction of the space of solutions to those with small amplitude, a standard technique in the analysis of nonlinear equations [13]. This section may be omitted by the reader not interested in the technical de-

*Electronic address: t.b.liverpool@leeds.ac.uk

 ©2005 The American Physical Society

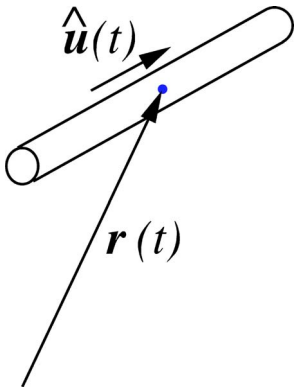

FIG. 1. (Color online) The degrees of freedom $(\mathbf{r},\hat{\mathbf{u}})$ associated with Brownian dynamics of a rod.

tails of the calculation who can skip to Sec. IV where the results for various correlation functions are presented and compared with previous results. Finally we discuss the results and perspectives in Sec. V

II. DYNAMICS OF WORMLIKE CHAINS

A. Fluctuating dynamics of rods

To understand the dynamics of a link of fixed length it is useful to consider the dynamics of a rod of length ℓ and diameter b (see Fig. 1). A dimer-rod at time t is described by an orientation given by a unit vector, $\hat{\mathbf{u}}(t)$, and position $\mathbf{r}(t)$ which both undergo Brownian motion [1,27–30] (and with the orientational dynamics satisfying the constraint of unit magnitude of $\hat{\mathbf{u}}$ [31–36]),

$$\partial_t \hat{\mathbf{u}} = \tilde{\zeta}_u^{-1} \hat{\mathbf{u}} \times \mathbf{f}(t), \quad \hat{\mathbf{u}} \cdot \partial_t \hat{\mathbf{u}} = 0, \tag{1}$$

$$\underline{\underline{\zeta}} \cdot \partial_t \mathbf{r} = \mathbf{g}(t), \tag{2}$$

where the random torques and forces are given by the three-dimensional vectors with

$$\langle \mathbf{f}(t) \rangle = 0, \quad \langle f_i(t) f_j(t') \rangle = 2T\tilde{\zeta}_u \delta_{ij} \delta(t-t'), \tag{3}$$

$$\langle \mathbf{g}(t) \rangle = 0, \quad \langle g_i(t) g_j(t') \rangle = 2T\tilde{\zeta}_{ij} \delta(t-t'), \tag{4}$$

in units where $k_B=1$. The rotational friction $\tilde{\zeta}_u \sim \eta\ell^3/3\ln(\ell/b)$ [1] and translational friction tensor is $\underline{\underline{\tilde{\zeta}}} = \hat{\mathbf{u}}\hat{\mathbf{u}}\tilde{\zeta}_\parallel + (\boldsymbol{\delta} - \hat{\mathbf{u}}\hat{\mathbf{u}})\tilde{\zeta}_\perp$ with transverse $[\tilde{\zeta}_\perp \sim \eta\ell/\ln(\ell/b)]$ and longitudinal $\left(\tilde{\zeta}_\parallel \simeq \frac{1}{2}\tilde{\zeta}_\perp\right)$ components. We note that $\mathbf{f}(t)$ is a pseudovector [40] and can therefore be written as $\mathbf{f}(t) = \mathbf{f}(t) \times \hat{\mathbf{u}}$ and the Langevin equation (1) can be rewritten in the form

$$\tilde{\zeta}_u \partial_t \hat{\mathbf{u}} = (\boldsymbol{\delta} - \hat{\mathbf{u}}\hat{\mathbf{u}}) \cdot \mathbf{f}(t). \tag{5}$$

where the correlations of $\mathbf{f}(t)$ are the same as $\mathbf{f}(t)$ [41].

Starting from the stochastic partial differential equation corresponding to the Langevin equation for $\hat{\mathbf{u}}$, Eq. (1) it is relatively straightforward to obtain the (equivalent) "diffusion" equation for the probability $P(\hat{\mathbf{n}},t)$ that the orientation at time t is $\hat{\mathbf{n}}$, $\partial_t P = D_r \vec{\mathcal{R}}^2 P$, where $\vec{\mathcal{R}} = \hat{\mathbf{n}} \times \partial_{\hat{\mathbf{n}}}$ and $D_r = T/\tilde{\zeta}_u$ [30,37–39]. A demonstration is sketched in Appendix A. It corresponds to Brownian motion on the surface of the unit sphere, $\mathcal{S}_2$. Starting with Eq. (1), one can also calculate explicitly the dynamic correlation function $\langle \hat{\mathbf{u}}(t) \cdot \hat{\mathbf{u}}(0) \rangle = \exp(-2D_r t)$. By construction, we have two orientational and three translational degrees of freedom [37].

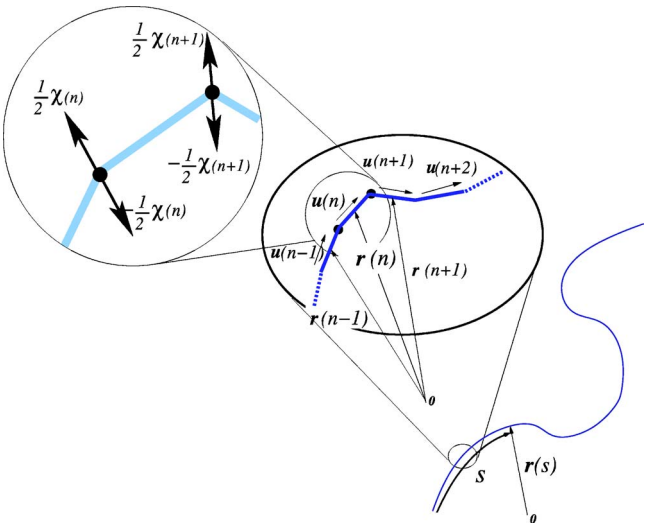

FIG. 2. (Color online) The wormlike chain as a limit of a chain of links of orientation $\hat{\mathbf{u}}(n)$ and position $\mathbf{r}(n)$. The continuous limiting curve $\mathbf{r}(s)$ where $s=\ell n$.

B. Fluctuating dynamics of WLC's

Historically, the wormlike chain model for semiflexible polymers was proposed (in equilibrium) as a continuum limit $(\ell/L \to 0)$ of a jointed chain (total length L) of links of length ℓ with a "bending" potential between neighboring links which are not parallel [4]. A schematic is shown in Fig. 2. The wormlike chain can be parametrized by the position vector $\mathbf{r}(s)$ and has a bending energy Hamiltonian

$$\mathcal{H} = \frac{A}{2} \int_0^L ds (\partial_s \hat{\mathbf{u}})^2 \tag{6}$$

and *two* constraints (1) $\hat{\mathbf{u}}(s) = \partial_s \mathbf{r}(s) \Leftrightarrow$ connectivity and (2) $|\hat{\mathbf{u}}(s)|^2 = 1 \Leftrightarrow$ inextensibility. Many equilibrium properties can be obtained by describing the chain in terms of the local unit tangent $\hat{\mathbf{u}}(s)$ [42,43]. However, as we discuss below, for dynamical properties imposing both constraints turns out to be a rather difficult and subtle procedure.

It is therefore very natural (and turns out to be rather illuminating) to consider the dynamics of a wormlike chain by taking the continuum limit of the *dynamics* of a chain of rodlike *links* of length ℓ. It is important to understand that the links here are coarse-grained entities which exist on much longer length scales than the chemical bonds which microscopically hold the chain together. In order to derive the dynamics of the filament we define the enthalpic functional G starting from the Hamiltonian in Eq. (6):

$$G[\hat{\mathbf{u}}(s),\mathbf{r}(s)] = \mathcal{H} + \int_0^L \boldsymbol{\chi}\cdot(\partial_s\mathbf{r} - \hat{\mathbf{u}})ds, \tag{7}$$

where the (vectorial) Lagrange multiplier function $\boldsymbol{\chi}(s)$ is used to enforce the constraint of connectivity—i.e., that $\partial_s\mathbf{r} = \hat{\mathbf{u}}$. The dynamics is determined by the variation of the functional δG with respect to variations $\delta\hat{\mathbf{u}}$ and $\delta\mathbf{r}$ [44,45]. The functions $\hat{\mathbf{u}}(s)$ and $\mathbf{r}(s)$ of s which we describe the chain can be approximated by continuous functions on scales above the "microscopic" length scale ℓ (compare, e.g., the Rouse model of flexible polymer dynamics [46]). The enthalpic contribution to the torque on the link at s is given by $\hat{\mathbf{u}}(s) \times -\delta G/\delta\hat{\mathbf{u}}(s)$ [1,27] while the enthalpic contribution to the force on the link is given by $-\delta G/\delta\mathbf{r}(s)$. From slender body hydrodynamics at low Reynolds number, we calculate the viscous torque due to an angular velocity $\boldsymbol{\omega}_{\hat{\mathbf{u}}}$ as given by $\tilde{\zeta}_u\boldsymbol{\omega}_{\hat{\mathbf{u}}}$ where $\boldsymbol{\omega}_{\hat{\mathbf{u}}}$ is by definition perpendicular to $\hat{\mathbf{u}}$. Similarly the viscous force due to a velocity $\partial_t\mathbf{r}$ as given by $\{\hat{\mathbf{u}}(s)\hat{\mathbf{u}}(s)\tilde{\zeta}_\parallel + [\boldsymbol{\delta} - \hat{\mathbf{u}}(s)\hat{\mathbf{u}}(s)]\tilde{\zeta}_\perp\}\cdot\partial_t\mathbf{r}$. As a result of thermal fluctuations, there are random torques and forces on each link. The equations of motion are obtained from the balance of forces *and* torques on each on each infinitesimal element. It is useful to rescale the drag coefficients by the length of a link, ℓ, to get $\zeta_\perp = \ell^{-1}\tilde{\zeta}_\perp \propto \eta$, $\zeta_\parallel = \ell^{-1}\tilde{\zeta}_\parallel \propto \eta$, and $\zeta_u = \ell^{-1}\tilde{\zeta}_u \propto \eta\ell^2$.

(i) Torque balance

$$\partial_t\hat{\mathbf{u}}(s,t) = \zeta_u^{-1}\hat{\mathbf{u}} \times ([A\partial_s^2\hat{\mathbf{u}} + \boldsymbol{\chi}(s,t)] \times \hat{\mathbf{u}} + \mathbf{f}(s,t)), \tag{8}$$

which maintains $\hat{\mathbf{u}}$ as a unit vector

$$\hat{\mathbf{u}}\cdot\partial_t\hat{\mathbf{u}}(s,t) = 0. \tag{9}$$

(ii) Force balance

$$\underline{\underline{\boldsymbol{\zeta}}}\cdot\partial_t\mathbf{r}(s,t) = \partial_s\boldsymbol{\chi} + \mathbf{g}(s,t), \tag{10}$$

with the constraint that

$$\hat{\mathbf{u}} = \partial_s\mathbf{r}, \tag{11}$$

linking Eqs. (8) and (10) and determining $\boldsymbol{\chi}$. The local friction tensor is given by

$$\underline{\underline{\boldsymbol{\zeta}}}(s) = \hat{\mathbf{u}}(s)\hat{\mathbf{u}}(s)\zeta + [\boldsymbol{\delta} - \hat{\mathbf{u}}(s)\hat{\mathbf{u}}(s)]\zeta_\perp.$$

Putting together Eqs. (8) and (9) and expressing the random torques (pseudovector) in terms of random forces with the same correlations [41], $\mathbf{f}(s,t) = \mathbf{f}(s,t)\times\hat{\mathbf{u}}(s,t)$, we get an alternative formulation in terms of the coupled dynamical equations:

$$\zeta_u\partial_t\hat{\mathbf{u}} = (\boldsymbol{\delta} - \hat{\mathbf{u}}\hat{\mathbf{u}})\cdot[A\partial_s^2\hat{\mathbf{u}} + \boldsymbol{\chi} + \mathbf{f}(s,t)], \tag{12}$$

$$\underline{\underline{\boldsymbol{\zeta}}}\cdot\partial_t\mathbf{r}(s,t) = \partial_s\boldsymbol{\chi} + \mathbf{g}(s,t), \tag{13}$$

$$\hat{\mathbf{u}}(s,t) = \partial_s\mathbf{r}(s,t), \tag{14}$$

where Eq. (14) determines the *local* connectivity *force* $\boldsymbol{\chi}(s,t)$. We note that this formulation is particularly convenient for simulations [43]. Equations (8), (10), and (12)–(14) are the first novel results of this paper and constitute a new and alternative way to analyze the dynamics of inextensible filaments. In the following sections we will use them to analyze the fluctuating dynamics of single filaments but they can also be used to calculate the rheological properties of semiflexible filament solutions [5,43].

The connectivity forces $\boldsymbol{\chi}(s,t)$ can also be thought of as contact forces [48] on the ends of the links which maintain the connectivity of the chain (see Fig. 2). The viscous torque on left-hand side (LHS) of Eq. (12) is balanced by the torques due to elastic (bending), connectivity, and thermal forces on the RHS. In Eq. (13), the viscous forces are balanced by connectivity and thermal forces. The value of the *fluctuating* connectivity force is given by the connectivity constraint, Eq. (14). While Eq. (8) bears some superficial similarity to the Landau-Lifshitz equation for the dynamics of spins in a ferromagnet [49] it is fundamentally different because of the constraint that the "spins" remain "connected." The *fluctuating* connectivity force $\boldsymbol{\chi}(s,t)$ leads to completely different physics.

The random forces $\mathbf{f}$ and $\mathbf{g}$ are Gaussian with zero mean—i.e.,

$$\langle\mathbf{f}(s,t)\rangle = \langle\mathbf{g}(s,t)\rangle = 0$$

and

$$\langle f_i(s,t)f_j(s',t')\rangle = 2T\ell^{-1}\zeta_u\delta_{ij}\delta(t-t')\delta(s-s'),$$

$$\langle g_i(s,t)g_j(s',t')\rangle = 2T\zeta_{ij}(s)\delta_{ij}\delta(t-t')\delta(s-s').$$

For simplicity in the following sections we will ignore the difference between longitudinal and transverse friction and use a scalar isotropic friction $\zeta = (1/3)(2\zeta_\perp + \zeta_\parallel)$. It is straightforward but cumbersome to include an anisotropic friction.

The variations of G with respect to $\mathbf{r}$, $\hat{\mathbf{u}}$ also specify the boundary conditions at the ends of the filament. For force- and torque-free ends of the filament they are

$$\partial_s\hat{\mathbf{u}}(0) = \partial_s\hat{\mathbf{u}}(L) = 0, \quad \boldsymbol{\chi}(0) = \boldsymbol{\chi}(L) = 0. \tag{15}$$

Alternative boundary conditions such as a clamped or hinged end are also simple to implement.

We note that we have just two degrees of freedom for each link and an additional three degrees of freedom for the center of mass of the whole filament. The obvious advantage of this description to the usual generalized coordinates such as link (bond) angles is that the equations of motion here are given in terms of the Cartesian vectors $\mathbf{u}(s,t)$ and $\mathbf{r}(s,t)$. We also emphasize that the "connectivity force" is also a requirement of any description using link angles because rotation of a particular link necessarily requires translation of the neighboring links in order to satisfy chain connectivity. The translation of these links necessarily dissipates energy because of the friction of the solvent. In other words there must be a dissipative time scale associated with the propagation of disturbances along the chain. Therefore a description solely in terms of the link angles is *not* sufficient to describe inextensible chain dynamics.

C. Taking the "continuum" limit: comparison to standard formulation

It is illuminating to take the "continuum" limit obtained by keeping only the the leading- (lowest-) order term in an expansion in ℓ/L for finite values of L [46]. Rewriting Eq. (12) in terms of the dimensionless arclength $\hat{s}=s/L$ and using the definition of the friction coefficients, $\zeta_u \propto \eta\ell^2$, and hence $\langle f_i f_j\rangle \propto \zeta_u$ allows one to simplify the dynamical equation (12) for $\hat{\mathbf{u}}$. Since the dynamics for $\hat{\mathbf{u}}$ no longer constrains it to be a unit vector, another constraint is needed. Equation (12) becomes

$$\mathbf{0} = (\boldsymbol{\delta} - \hat{\mathbf{u}}\hat{\mathbf{u}}) \cdot [A\partial_s^2 \hat{\mathbf{u}} + \boldsymbol{\chi}(s,t)], \tag{16}$$

$$1 = \hat{\mathbf{u}}^2. \tag{17}$$

It is convenient to decompose the connectivity force into components perpendicular (transverse) and parallel (longitudinal) to the local tangent,

$$\boldsymbol{\chi}(s,t) = \boldsymbol{\chi}_\perp(s,t) + \hat{\mathbf{u}}\chi_\parallel(s,t),$$

where

$$\boldsymbol{\chi}_\perp(s,t) = (\boldsymbol{\delta} - \hat{\mathbf{u}}\hat{\mathbf{u}}) \cdot \boldsymbol{\chi}, \quad \chi_\parallel(s,t) = \hat{\mathbf{u}} \cdot \boldsymbol{\chi}, \tag{18}$$

and from Eq. (16) we obtain an expression for the transverse component of $\boldsymbol{\chi}$, but find the longitudinal component unconstrained,

$$\boldsymbol{\chi}_\perp = -A\partial_s^2 \hat{\mathbf{u}} + A(\hat{\mathbf{u}}\hat{\mathbf{u}} \cdot \partial_s^2 \hat{\mathbf{u}}) \tag{19}$$

and hence

$$\partial_s \boldsymbol{\chi} = \partial_s(\hat{\mathbf{u}}\chi_\parallel) - A\partial_s^3 \hat{\mathbf{u}} + \partial_s[A\hat{\mathbf{u}}\hat{\mathbf{u}} \cdot \partial_s^2 \hat{\mathbf{u}}]. \tag{20}$$

Substituting Eq. (20) into Eq. (13) and implementing the connectivity constraint, Eq. (14), we obtain

$$\underline{\underline{\boldsymbol{\zeta}}} \cdot \partial_t \mathbf{r} = -A\partial_s^4 \mathbf{r} + \partial_s[\partial_s \mathbf{r}(A\partial_s \mathbf{r} \cdot \partial_s^3 \mathbf{r} + \chi_\parallel)] + \mathbf{g}(s,t), \tag{21}$$

$$1 = |\partial_s \mathbf{r}|^2, \tag{22}$$

where the constraint in Eq. (22) fixes the value of $\chi_\parallel(s,t)$

In general the wormlike chain Hamiltonian is written as

$$\mathcal{H}_{\mathrm{wlc}}[\{\mathbf{r}(s)\}] = \frac{A}{2}\int_0^L ds(\partial_s^2 \mathbf{r})^2. \tag{23}$$

The connectivity constraint is implicit in this definition and inextensibility is implemented by the constraint that the tangent vector $\partial_s \mathbf{r}$ is a unit vector. We can define an alternative enthalpic functional [44,45]

$$G'[\mathbf{r}(s)] = \mathcal{H}_{\mathrm{wlc}} + \int_0^L ds\,\tau|\partial_s \mathbf{r}|^2, \tag{24}$$

where the (scalar) Lagrange multiplier $\tau(s)$, the *tension*, is used to enforce the constraint of inextensibility—i.e., that $(\partial_s \mathbf{r})^2 = 1$. The dynamics is determined by the variation of the functional $\delta G'$ with respect to variations $\delta\mathbf{r}$ [44,45]. We impose force balance on each element of the filament, leading to the dynamical equations

$$\underline{\underline{\boldsymbol{\zeta}}} \cdot \partial_t \mathbf{r}(s,t) = -A\partial_s^4 \mathbf{r} + \partial_s(\tau(s,t)\partial_s \mathbf{r}) + \mathbf{f}(s,t), \tag{25}$$

$$1 = |\partial_s \mathbf{r}|^2. \tag{26}$$

There is only one *nonlinear* equation but a *nonlinear* constraint. The thermal fluctuations are given by $\langle \mathbf{f}(s,t)\rangle = 0$ and $\langle f_i(s,t) f_j(s',t')\rangle = 2T\zeta_{ij}\delta(s-s')\delta(t-t')$. Comparison of Eq. (25) with Eq. (21) shows that the Lagrange multiplier for inextensibility (the tension) is given in terms of the connectivity force $\boldsymbol{\chi}$ by

$$\tau(s,t) = A\partial_s \mathbf{r} \cdot \partial_s^3 \mathbf{r} + \partial_s \mathbf{r} \cdot \boldsymbol{\chi}(s,t), \tag{27}$$

thus making an explicit link to the standard formulation of semiflexible polymer dynamics.

The motivation for this formulation of semiflexible filament dynamics lies in the fact that the dynamics is *intrinsically* locally length preserving. In this section we have seen that taking the continuum limit [46] at the level of the equations of motion reduces to the standard formulation and loses this property. In the following section we will perform a calculation for which we take the limit at the end of the calculation.

While both the equation and the constraint of the standard description are nonlinear [see Eqs. (25) and (26)], in the new approach, the nonlinearity occurs only in Eq. (12) and is purely *geometric* in nature. The chain dynamics presented here corresponds to a diffusive process on the surface of a sphere coupled to diffusion in three-dimensional space.

III. EXPLICIT ANALYSIS

Much of the recent progress in describing the dynamics of semiflexible filaments analytically has been performed by making a *small-amplitude expansion* of the bending fluctuations about a *stationary* rodlike conformation (the so-called weakly bending rod limit) [6,50,51]. This is expected to be valid for chains shorter than the persistence length. A description of the dynamics obtained by expanding about a stationary reference state is a reasonable approximation for times much shorter than the typical rotation or translation time of the filaments) [6,50,51].

In this section using the dynamical equations developed in the previous section, we attempt to extend this approach to consider the dynamics on time scales up to and exceeding the global rotation and translation time of the filaments. We do this by expanding around not a *stationary* reference state but one which is *dynamic*. It emerges naturally out of the new formulation how this state should be chosen and we find that, within our approximations, the fluctuations about this state remain small for all times. For short time scales, the results reduce to those obtained earlier from expansions about stationary reference states. It is expected that the results will be useful for analyzing dynamical experiments on semiflexible filaments like F-actin such as video microscopy [50] and scattering experiments [16,51,52]

Starting from Eqs. (12)–(14), we now present a self-consistent calculation of the dynamics of all the modes of a chain of fixed length which can be systematically improved and shows how internal and global modes mix and hence how to separate the two types of motion.

We consider chains of length $L < L_p = A/T$ so that the chain has a well-defined average orientation given by the

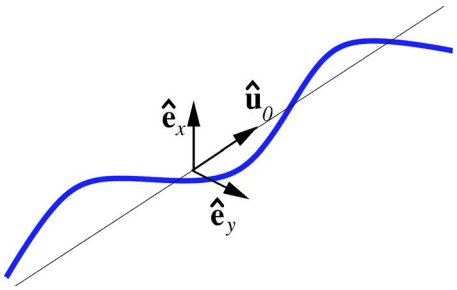

FIG. 3. (Color online) The local frame for filament dynamics.

unit vector $\hat{\mathbf{u}}_0(t)$. We can w.l.g. write the local orientation in terms of the mean orientation

$$\hat{\mathbf{u}}(s,t) = \hat{\mathbf{u}}_0(t) + \delta\mathbf{u}(s,t). \tag{28}$$

The orientation vector defines a right-hand set of axes (see Fig. 3) which we call *the instantaneous "Monge" frame* which is *parallel transported* forward in time by $\hat{\mathbf{u}}_0$, $\{\hat{\mathbf{e}}_x(t), \hat{\mathbf{e}}_y(t), \hat{\mathbf{u}}_0(t)\}$ and we can write

$$\delta\mathbf{u}(s,t) = u_x(s,t)\hat{\mathbf{e}}_x(t) + u_y(s,t)\hat{\mathbf{e}}_y(t) + u_z(s,t)\hat{\mathbf{u}}_0(t). \tag{29}$$

The mean orientation is defined as $\hat{\mathbf{u}}_0(t) = \int_0^L ds\hat{\mathbf{u}}(s,t)/|\int_0^L ds\hat{\mathbf{u}}(s,t)|$. Applying the connectivity constraint, Eq. (14), to Eq. (29), we can also w.l.g. write the filament position as

$$\mathbf{r}(s,t) = \mathbf{r}(0,t) + [s + r_z(s,t)]\hat{\mathbf{u}}_0 + r_x(s,t)\hat{\mathbf{e}}_x + r_y(s,t)\hat{\mathbf{e}}_y, \tag{30}$$

where $\mathbf{r}(0,t)$ is the position of one end of the filament and $r_i(s,t) = \int_0^s u_i(s',t)\mathrm{d}s' \Rightarrow u_i = \partial_s r_i$, where $i \in \{x,y,z\}$.

We denote $u_x(s,t)$ and $u_y(s,t)$ as the transverse components of the local orientation and $u_z(s,t)$ as the longitudinal component.

The small-amplitude approximation amounts to considering only those solutions of the equations which can be described by small perturbations around a rigid rod of orientation $\hat{\mathbf{u}}_0(t)$. Such a description is *not* a systematic expansion in a small parameter of the equations but rather a *restriction* of the space of solutions to those which have small amplitude [13]. The solutions obtained within this approximation can then be checked *a posteriori*. Therefore we write the transverse components

$$\begin{pmatrix} u_x \\ u_y \end{pmatrix} = \epsilon \begin{pmatrix} v_x \\ v_y \end{pmatrix}, \tag{31}$$

where $v_i = O(1)$ for $i \in \{x,y\}$ and the small parameter ϵ measures the amplitude of the fluctuations about a rigid rod conformation. As $L/L_p \to 0$ it is expected that $\epsilon \to 0$.

Since $\hat{\mathbf{u}}$ is a unit vector,

$$u_z = -\frac{1}{2}(u_x^2 + u_y^2) + O(u_x^4), \tag{32}$$

so that $u_z = O(\epsilon^2)$. Equivalently,

$$\partial_t u_z = -(u_x\partial_t u_x + u_y\partial_t u_y) + O(\epsilon^4). \tag{33}$$

Since there are no constraints on $\boldsymbol{\chi}$, then $\boldsymbol{\chi} = O(1)$. From the definition of $r_i(s,t)$ above, $r_x/L = O(\epsilon)$, $r_y/L = O(\epsilon)$, and $r_z/L = O(\epsilon^2)$.

The dynamics at lowest order in ϵ, $O(1)$, is just that of a rigid rod of length L characterized by its center of mass $\mathbf{r}_0(t)$ and orientation $\hat{\mathbf{u}}_0(t)$ (see Sec. II A):

$$\frac{1}{3}\zeta L^3 \partial_t \hat{\mathbf{u}}_0 = (\boldsymbol{\delta} - \hat{\mathbf{u}}_0\hat{\mathbf{u}}_0)\cdot\mathbf{f}_0(t) + O(\epsilon), \tag{34}$$

$$L\zeta\partial_t \mathbf{r}_0 = \mathbf{g}_0(t) + O(\epsilon), \tag{35}$$

with random forces given by

$$\langle \mathbf{f}_0(t)\rangle = 0, \quad \langle f_{0i}(t) f_{0j}(t')\rangle = 2T\frac{L^3\zeta}{3}\delta_{ij}\delta(t-t'), \tag{36}$$

$$\langle \mathbf{g}_0(t)\rangle = 0, \quad \langle g_{0i}(t) g_{0j}(t')\rangle = 2TL\zeta\delta_{ij}\delta(t-t'), \tag{37}$$

where we have identified $\mathbf{g}_0(t) = \int_0^L ds\, \mathbf{g}(s,t)$ and $\mathbf{f}_0(t) = 2\int_0^L ds\, s[\mathbf{g}(s,t) - (1/L)\mathbf{g}_0(t)]$.

The position of the center of mass is defined as $\mathbf{r}_0(t) = (1/L)\int_0^L \mathbf{r}(s,t)ds$. To lowest order in ϵ,

$$\mathbf{r}_0(t) = \mathbf{r}(0,t) + \frac{L}{2}\hat{\mathbf{u}}_0(t) + O(\epsilon). \tag{38}$$

For a particular global orientation $\hat{\mathbf{u}}_0(t)$ and position $\mathbf{r}_0(t)$ whose dynamics follows Eqs. (34) and (35), we now study the dynamics of the internal modes independently of the global rotation and translation modes.

We now consider the equations to the next order in ϵ taking account of the internal (bending) modes. Using Eqs. (12), (13), (34), and (35) we can obtain dynamical equations for $\delta\mathbf{u}$ and $\mathbf{r}$. The internal modes to first order in ϵ are given by the dynamics in the two-dimensional space of fluctuations transverse to $\hat{\mathbf{u}}_0$, since $u_z = \partial_s r_z$ is of order $O(\epsilon^2)$ from Eq. (33). Therefore $\delta\mathbf{u} = \hat{\mathbf{u}}(s,t) - \hat{\mathbf{u}}_0(t) = \mathbf{U} + O(\epsilon^2)$ which we write in terms of $\{\hat{\mathbf{e}}_x(t), \hat{\mathbf{e}}_y(t)\}$ as

$$\mathbf{U}(s,t) = u_x\hat{\mathbf{e}}_x + u_y\hat{\mathbf{e}}_y \equiv \partial_s\mathbf{R}, \tag{39}$$

defining the vector $\mathbf{R}(s,t) = r_x\hat{\mathbf{e}}_x + r_y\hat{\mathbf{e}}_y$

Similarly from the definition of the Monge frame we can write

$$\boldsymbol{\chi}(s,t) = \chi_x\hat{\mathbf{e}}_x + \chi_y\hat{\mathbf{e}}_y + \chi_z\hat{\mathbf{u}}_0 \equiv \mathbf{X}(s,t) + \chi_z\hat{\mathbf{u}}_0, \tag{40}$$

$$\mathbf{f}(s,t) = f_x\hat{\mathbf{e}}_x + f_y\hat{\mathbf{e}}_y + f_z\hat{\mathbf{u}}_0 \equiv \mathbf{F}(s,t) + f_z\hat{\mathbf{u}}_0, \tag{41}$$

$$\mathbf{g}(s,t) = g_x\hat{\mathbf{e}}_x + g_y\hat{\mathbf{e}}_y + g_z\hat{\mathbf{u}}_0 \equiv \mathbf{G}(s,t) + g_z\hat{\mathbf{u}}_0, \tag{42}$$

defining the transverse vectors $\mathbf{X}(s,t)$, $\mathbf{F}(s,t)$, and $\mathbf{G}(s,t)$.

Expanding Eqs. (12) and (13) to $O(\epsilon)$, we get the dynamical equations for $\mathbf{U}$ and $\mathbf{R}$,

$$\zeta_u\partial_t\mathbf{U}(s,t) = A\partial_s^2\mathbf{U} + \chi_z\mathbf{U} + \mathbf{X} + \mathbf{F} - \frac{3\zeta_u}{\zeta L^3}\boldsymbol{\Phi}_0, \tag{43}$$

$$\zeta\partial_t\mathbf{R}(s,t) = \partial_s\mathbf{X} + \mathbf{G} - \frac{1}{L}\mathbf{\Gamma}_0 - \frac{3(2s-L)}{2L^3}\Phi_0, \tag{44}$$

where $\mathbf{\Phi}_0(t)=(\boldsymbol{\delta}-\hat{\mathbf{u}}_0\hat{\mathbf{u}}_0)\cdot\mathbf{f}_0$ and $\mathbf{\Gamma}_0(t)=(\boldsymbol{\delta}-\hat{\mathbf{u}}_0\hat{\mathbf{u}}_0)\cdot\mathbf{g}_0$ are the transverse components of $\mathbf{f}_0(t)$ and $\mathbf{g}_0(t)$, respectively, defined in Eqs. (36) and (37).

In order to perform explicit calculations, we write Eqs. (43) and (44) in terms of the components of the basis vectors of the Monge frame, taking account of frame dynamics—i.e., $\partial_t\hat{\mathbf{e}}_i(t)\neq 0$. Defining $\mathbf{U}(s,t)\equiv(u_x,u_y)=\partial_s\mathbf{R}$, where $\mathbf{R}(s,t)=(r_x,r_y)$, and the two-dimensional (2d) vectors $\mathbf{X}(s,t)=(\chi_x,\chi_y)$, $\mathbf{F}(s,t)=(f_x,f_y)$, and $\mathbf{G}(s,t)=(g_x,g_y)$ we obtain

$$\zeta_u D_t\mathbf{U}(s,t) = A\partial_s^2\mathbf{U} + \chi_z\mathbf{U} + \mathbf{X} + \mathbf{F} - \frac{3\zeta_u}{\zeta L^3}\mathbf{\Phi}_0, \tag{45}$$

$$\zeta D_t\mathbf{R}(s,t) = \partial_s\mathbf{X} + \mathbf{G} - \frac{1}{L}\mathbf{\Gamma}_0 - \frac{3(2s-L)}{2L^3}\Phi_0, \tag{46}$$

with the covariant differential operator $D_t=\partial_t+f_{0z}\mathbb{S}$, where

$$\mathbb{S} = \begin{pmatrix} 0 & -1 \\ 1 & 0 \end{pmatrix}$$

and $f_{0z}=\hat{\mathbf{u}}_0\cdot\mathbf{f}_0$. In the following we replace it by its average $\langle D_t\rangle$.

To study the dynamics of r_z we must consider terms of $O(\epsilon^2)$. From Eq. (13), we obtain the equation of motion for r_z, the component of $\mathbf{r}$ in the direction of $\hat{\mathbf{u}}_0$,

$$\zeta\partial_t r_z = \partial_s\chi_z + g_z. \tag{47}$$

We note that from Eqs. (33) and (47), $\partial_s^2\chi_z+\partial_s g_z=O(\epsilon^2)$.

Given the boundary conditions, Eq. (15), we can expand $\delta\hat{\mathbf{u}}(s,t)$ in terms of the orthonormal basis functions,

$$\phi_p(s) = \left(\frac{2}{L}\right)^{1/2}\cos\left(\frac{p\pi s}{L}\right), \quad p\geqslant 1 \quad \text{and} \quad \phi_0(s) = \left(\frac{1}{L}\right)^{1/2},$$

$$\delta\hat{\mathbf{u}}(s,t) = \sum_{p=0}^{\infty}\tilde{\mathbf{u}}_p(t)\phi_p(s), \tag{48}$$

where $\mathbf{u}_p(t)=\mathbf{U}_p(t)+u_{zp}(t)\hat{\mathbf{u}}_0$ and $\mathbf{U}_p(t)=\int_0^L ds\ \mathbf{U}(s,t)\phi_p(s)$, $u_{zp}(t)=\int_0^L ds\ u_z(s,t)$. We can *define* $\mathbf{X}_p=\int_0^L ds\ \mathbf{X}(s,t)\phi_p(s)$, $\mathbf{F}_p=\int_0^L ds\ \mathbf{F}(s,t)\phi_p(s)$, and similarly $\mathbf{G}_p$.

Connectivity, Eq. (14), which means that $\mathbf{U}(s,t)=\partial_s\mathbf{R}(s,t)$, implies

$$\mathbf{R}(s,t) = \mathbf{R}_0(t) + \mathbf{U}_0(t)s\phi_0 + \sum_{p=1}^{\infty}\mathbf{R}_p(t)\psi_p(s), \tag{49}$$

where

$$\psi_p(s) = \left(\frac{2}{L}\right)^{1/2}\sin\left(\frac{p\pi s}{L}\right) \quad \mathbf{R}_p(t) = \frac{L}{p\pi}\mathbf{U}_p(t), \quad p\geqslant 1.$$

We note that the new formulation has two sets of basis functions which diagonalize two second-order differential equations in comparison to the standard approach with one set of basis functions diagonalizing one fourth-order differential equation as we solve two coupled second-order differential equations rather than one fourth-order equation [44].

The problem is solved in two steps. Taking into account the boundary conditions, Eq. (15), we expand the function $\chi_z(s,t)=\Sigma_{p=1}\chi_p(t)\psi_p(s)$ in modes. Defining $\hat{q}=q\pi/L$ and using Eqs. (15), (43), and (44), we obtain ($p\geqslant 1$)

$$\zeta\partial_t\mathbf{U}_p = -\hat{p}^2\mathbf{X}_p + \hat{p}\mathbf{G}_p + \boldsymbol{\gamma}_p(t), \tag{50}$$

$$\zeta_u\partial_t\mathbf{U}_p = -A\hat{p}^2\mathbf{U}_p + \sum_{k,q}\Omega_{kqp}\chi_k\mathbf{U}_q + \mathbf{X}_p + \mathbf{F}_p, \tag{51}$$

where

$$\Omega_{kpq} = \int_0^L ds\,\phi_p(s)\phi_q(s)\psi_k(s)$$

and

$$\boldsymbol{\gamma}_p(t) = \zeta 2^{1/2}\left(\cos p\pi\partial_t\mathbf{U}_0 - \frac{[1-\cos p\pi]}{L^{1/2}}\partial_t\mathbf{R}_0\right).$$

The internal modes of mode number p are coupled to the global modes by $\boldsymbol{\gamma}_p(t)$.

We can solve Eqs. (51) and (50) by taking Fourier transforms in time, $\mathbf{U}_p(\omega)=\int_{-\infty}^{\infty}dt\,e^{-i\omega t}\mathbf{U}_p(t)$, and eliminating $\mathbf{X}_p(\omega)$ to obtain the matrix equation

$$\sum_{q=1}^{\infty}\int_{\omega'}\mathbb{L}_{pq}(\omega-\omega')\cdot\mathbf{U}_q(\omega') = \boldsymbol{\beta}_p(\omega), \tag{52}$$

where $\boldsymbol{\beta}_p(\omega)=\boldsymbol{\gamma}_p(\omega)+\hat{p}\mathbf{G}_p(\omega)+\hat{p}^2\mathbf{F}_p(\omega)$. If we take the limit $\ell/L\to 0$ and for $p\gg 1$, then $\boldsymbol{\beta}_p=\hat{p}\mathbf{G}_p$.

We have defined the matrix operator

$$\mathbb{L}_{pq}(\omega-\omega') = \mathbb{L}_p^{(0)}(\omega)\delta_{pq}\delta(\omega-\omega') + \Delta\mathbb{L}_{pq}(\omega-\omega'), \tag{53}$$

whose diagonal part (in p, ω space) is

$$\mathbb{L}_p^{(0)}(\omega) = (i\omega\zeta + A\hat{p}^4 + i\omega\zeta_u\hat{p}^2)\mathbb{I}. \tag{54}$$

The nondiagonal part

$$\Delta\mathbb{L}_{pq}(\omega-\omega') = -\hat{p}^2\sum_k\Omega_{kqp}\chi_k(\omega-\omega')\mathbb{I}, \tag{55}$$

where

$$\mathbb{I} = \begin{pmatrix} 1 & 0 \\ 0 & 1 \end{pmatrix}$$

is the 2×2 unit matrix.

Equation (52) is a *linear* equation for $\mathbf{U}_p$ albeit with an unspecified fluctuating linear operator $\mathbb{L}_p(\omega,\omega')$. The fluctuations come from $\chi_z(s,t)$ or equivalently $\Delta\mathbb{L}_p(\omega,\omega')$. We can make a *functional* fluctuation expansion of $\mathbb{L}$ around its steady nonfluctuating part $\mathbb{L}_p^{(0)}(\omega)$.

The functional expansion can be written formally as

$$\mathbb{L}(\chi) = \mathbb{L}_0 + \chi\cdot(\delta\mathbb{L}/\delta\chi)_{\chi=0} + O(\chi^2) \tag{56}$$

and can be inverted to give

$$\mathbb{L}^{-1}(\chi) = \mathbb{L}_0^{-1} - \mathbb{L}_0^{-1} \cdot \chi \cdot (\delta\mathbb{L}/\delta\chi)_{\chi=0} \cdot \mathbb{L}_0^{-1} + O(\chi^2), \quad (57)$$

where summation over p and integration over ω is implied. This expansion can be resummed by using it to calculate the fluctuations of $r_z(s,t)$ using Eqs. (14) and (33) and requiring that, for self-consistency [16], the result obtained must satisfy Eq. (47).

Defining $\Gamma_p = [\mathbb{L}_p^{(0)}]^{-1}$ and noting $\hat{p} = p\pi/L$, from inverting Eq. (52), we obtain

$$\mathbf{U}_q(\omega) = \Gamma_q(\omega) \cdot \boldsymbol{\beta}_q(\omega) + \hat{q}^2 \Gamma_q(\omega) \times \int_{\omega'} \sum_{k,p} \Omega_{kpq} \Gamma_p(\omega') \chi_k(\omega - \omega') \boldsymbol{\beta}_p(\omega'), \quad (58)$$

where we have taken the limit $\ell/L \to 0$. From Eq. (33) [defining $u_z(s,\omega) \equiv \int_t e^{i\omega t} u_z(s,t)$], we have the relationship

$$u_z(s,\omega) = -\frac{1}{2} \sum_{n,m} \phi_n(s) \phi_m(s) \int_{\omega'} \mathbf{U}_n(\omega - \omega') \cdot \mathbf{U}_m(\omega'). \quad (59)$$

Defining $\rho_z(\omega) \equiv r_z(L,\omega) - r_z(0,\omega)$, we obtain, using orthonormality of $\phi_p(s)$,

$$\rho_z(\omega) = -\frac{1}{2} \sum_n \int_{\omega'} \mathbf{U}_n(\omega - \omega') \cdot \mathbf{U}_n(\omega'). \quad (60)$$

Using Eq. (58), we obtain the *unaveraged* expression

$$\rho_z(\omega) = -\sum_n \alpha_n(\omega) - \sum_{n,k} \int_{\omega_1,\omega_2} \mathcal{J}_{kn}(\omega,\omega_1,\omega_2) \chi_k \times (\omega - \omega_1 - \omega_2). \quad (61)$$

The *fluctuating* functions $\mathcal{J}_{kn}(\omega,\omega_1,\omega_2)$ and $\alpha_k(\omega)$ are given by

$$\mathcal{J}_{kn}(\omega,\omega_1,\omega_2) = \hat{n}^2 \sum_p \Omega_{kpn} [\Gamma_n(\omega - \omega_1) \Gamma_n(\omega_1) \Gamma_p \times (\omega_2 - \omega) \boldsymbol{\beta}_p(\omega_2 - \omega) \cdot \boldsymbol{\beta}_n(\omega - \omega_1) + \Gamma_n(\omega_1) \Gamma_n(\omega - \omega_1) \Gamma_p(\omega_2) \boldsymbol{\beta}_p(\omega_2) \cdot \boldsymbol{\beta}_n(\omega_1)] \quad (62)$$

and

$$\alpha_k(\omega) = \int_{\omega'} \Gamma_k(\omega - \omega') \Gamma_k(\omega') \boldsymbol{\beta}_k(\omega - \omega') \cdot \boldsymbol{\beta}_k(\omega'). \quad (63)$$

We now impose the self-consistency condition, by substituting the result, Eq. (61), into Eq. (47). This leads to the *unaveraged* mode equation for the "connectivity" force $(n,k \geq 1)$:

$$-i\omega\zeta \left[\alpha_n(\omega) + \sum_k \int_{\omega_1,\omega_2} \mathcal{J}_{nk}(\omega,\omega_1,\omega_2) \chi_n(\omega - \omega_1 - \omega_2) \right] = \left(\frac{2}{L}\right)^{1/2} \hat{n} (\cos n\pi - 1) [\chi_n(\omega) + g_n(\omega)], \quad (64)$$

where $g_k(\omega) = \int_t e^{i\omega t} \int_s \phi_k(s) g_z(s,t)$. We emphasize that both functions α_k and $\mathcal{J}_{kn}$ on the LHS of Eq. (64) are fluctuating and depend on the thermal fluctuations given by $\boldsymbol{\beta}_p(\omega)$. Rearranging Eq. (64) we obtain the (self-consistent) equation for χ_n:

$$\int_{\omega_1,\omega_2} \frac{\chi_n(\omega - \omega_1 - \omega_2)}{\Gamma_n^{\chi}(\omega,\omega_1,\omega_2)} = \hat{n} g_n(\omega) + i\omega\zeta \left(\frac{L}{2}\right)^{1/2} \frac{\alpha_n(\omega)\hat{n}}{1 - \cos n\pi}, \quad (65)$$

where we have defined the *fluctuating* response function $\Gamma_n^{\chi}(\omega,\omega_1,\omega_2)$,

$$\frac{1}{\Gamma_n^{\chi}(\omega,\omega_1,\omega_2)} = \sum_k \left(\frac{L}{2}\right)^{1/2} \frac{\hat{n} \mathcal{J}_{nk}(\omega,\omega_1,\omega_2)}{\cos n\pi - 1} - \hat{n}^2 (2\pi)^2 \delta(\omega_1) \delta(\omega_2). \quad (66)$$

In Eqs. (58), (65), and (66), we have obtained an unaveraged *and* self-consistent theory for the chain dynamics taking into account inextensibility and connectivity. An important feature of such a theory is a fluctuating connectivity force (or tension). To proceed further—i.e., obtain an expression for the response function—we must invert the fluctuating linear operator $[\Gamma_k^{\chi}(\omega,\omega_1,\omega_2)]^{-1}$. However, in Eq. (66), we have a stochastic integrodifferential equation with both multiplicative colored noise (from $\mathcal{J}_{kn}$) and additive colored noise (from α_k, g_k). Because of the multiplicative noise, the operator cannot be inverted without further approximation. The required minimal approximation is an average of $[\Gamma_k^{\chi}(\omega,\omega_1,\omega_2)]^{-1}$ over the transverse fluctuations. Such an approximation is clearly uncontrolled; however, similar, *preaveraging* approximations have been used (with some success) in the dynamics of flexible polymers with hydrodynamic interactions [1]. There is a slight difference, however, as there the average is over an equilibrium distribution while here we average over dynamic fluctuations. This dynamic preaveraged approximation corresponds to assuming a separation of time scales between the longitudinal and transverse fluctuations which becomes a better approximation the more rigid the filament is. We emphasize that we average only Γ_k^{χ} and we *do not* perform an average of α_k over the transverse fluctuations yet (see later) as this will lead to the wrong long-time behavior. Keeping track of the fluctuations in α_k leads to a consistent picture of the behavior for the longitudinal fluctuations at intermediate times [16] which takes account of the finite time of tension propagation. Performing the average over β_k and changing the variable to $\theta_1 = \omega_1 + \omega_2$ and $\theta_2 = \omega_1 - \omega_2$, we obtain

$$\left\langle \sum_n \int_{\theta_2} \mathcal{J}_{kn}(\omega,\theta_1,\theta_2) \right\rangle = 2\pi\delta(\theta_1) \left(\frac{2}{L}\right)^{3/2} \frac{(1 - \cos k\pi)}{L_p \hat{k}} \times J_k(-i\omega\tau_1), \quad (67)$$

where

$$J_k(x) = \frac{\pi}{4x^{1/4}} \left[\frac{\cot \pi x^{1/4}}{(x^{1/2} - k^2/4)} + \frac{\coth \pi x^{1/4}}{(x^{1/2} + k^2/4)} \right], \quad (68)$$

and τ_1 is the relaxation-time longest-lived bending mode of the filament defined as $\tau_1^{-1} = 2A\pi^4/\zeta L^4$.

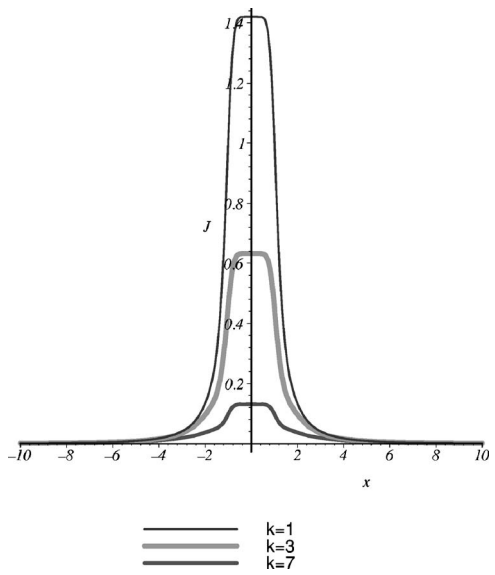

FIG. 4. The compliance $J_k(-i\omega\tau_1)$ plotted against $\omega\tau_1$ for the modes $k=1,3,7$.

The sum over modes of the compliance $\Sigma_k J_k(-i\omega\tau_1)$ can easily be evaluated and is closely related to the tension modulus, the part of the viscoelastic response of a dilute solution of semiflexible filaments coming from flow-induced tensions in the filament. We plot the form of $J_k(x)$ for different values of k in Fig. 4. The expression for $J_k(x)$ becomes simple in two limits for $\lim_{\omega\tau_1\gg 1} J_k(x) \simeq \pi x^{-3/4}/4$ and $\lim_{\omega\tau_1\ll 1} J_k(x) \simeq 2\pi^2/(3k^2)$.

From Eqs. (65)–(67), we obtain the *preaveraged* mode equation with the averaged inverse response function, for the "connectivity" force:

$$\chi_k(\omega) = \Gamma_k^{\chi}(\omega)\left[\hat{k} g_k(\omega) + i\omega\zeta \frac{\alpha_k(\omega)\hat{k}}{1-\cos k\pi}\right], \tag{69}$$

where we have defined the preaveraged response function $\Gamma_k^{\chi}(\omega)$,

$$\frac{1}{\Gamma_k^{\chi}(\omega)} = \left[-\hat{k}^2 + \frac{2}{L_p L}(-i\omega\tau_1) J_k(-i\omega\tau_1)\right]. \tag{70}$$

This leads to an equation for $\rho_z(\omega)$,

$$\rho_z(\omega) = \sum_k \Gamma_k^{\chi}(\omega)\left[-\hat{k}^2\alpha_k(\omega) + \frac{2^{3/2}\tau_1(1-\cos \pi k)}{L_p L^{3/2}\zeta} \times J_k(-i\omega\tau_1) g_k(\omega)\right], \tag{71}$$

from which we can calculate the mean excess length $\langle \rho_z(t)\rangle = \int_\omega \langle \rho_z(\omega)\rangle e^{-i\omega t}$. Since $\langle g_k(\omega)\rangle = 0$ (noting $\ell/L \to 0$), we average over α_k to get

$$\langle \rho_z(t)\rangle = -\frac{2L^2}{\pi^2 L_p}\sum_{m=1}^{\infty}\frac{1}{m^2} = -\frac{L^2}{3L_p}. \tag{72}$$

We now return to the dynamics of the global modes. From Eqs. (43) and (44) multiplying by $\phi_0(s)$ and $s\phi_0(s)$, respectively, and integrating over s from 0 to L, and using Eq. (49), we obtain the coupled equations which allows one to solve for $\mathbf{X}_0$, $\mathbf{R}_0$ and $\mathbf{U}_0$:

$$\zeta\left(L^{1/2}\partial_t \mathbf{R}_0 + \frac{L}{2}\partial_t \mathbf{U}_0 - \frac{\sqrt{2}}{L}\sum_{p=1}\left[\frac{(-1)^p - 1}{\hat{p}^2}\right]\partial_t \mathbf{U}_p\right) = \mathbf{0}, \tag{73}$$

$$\zeta\left(L^{1/2}\partial_t \mathbf{R}_0 + \frac{2L}{3}\partial_t \mathbf{U}_0 - 2\frac{\sqrt{2}}{L}\sum_{p=1}\left[\frac{(-1)^p}{\hat{p}^2}\right]\partial_t \mathbf{U}_p\right) = -\frac{2}{L}\mathbf{X}_0 + \frac{1}{2L^{3/2}}\mathbf{\Phi}_0, \tag{74}$$

$$\partial_t \mathbf{U}_0 = \frac{1}{\zeta_u}(\mathbf{X}_0 + \mathbf{F}_0) - \frac{3}{\zeta L^{5/2}}\mathbf{\Phi}_0, \tag{75}$$

where we have identified $\mathbf{\Gamma}_0(t) = \int_0^L ds\, \mathbf{G}(s,t)$ and $\mathbf{\Phi}_0(t) = 2\int_0^L ds\, s[\mathbf{G}(s,t) - (1/L)\mathbf{\Gamma}_0(t)]$. These equations together with Eqs. (34) and (35) give the dynamics of the global modes which are coupled to the internal modes of mode number $p \geqslant 1$.

Because of the $1/p^2$ dependence, the corrections due to the dynamics of the higher modes decrease as the mode number p increases. We can obtain progressively better approximations by including more and more modes. The zeroth-order approximation corresponds to ignoring all the modes with $p \geqslant 1$. In this case, we can straightforwardly calculate the dynamic correlation functions of $\mathbf{U}_0$, $\mathbf{R}_0$, and $\mathbf{u}_0$, which are given by

$$\frac{1}{L}\langle[\mathbf{U}_0(t) - \mathbf{U}_0(0)]^2\rangle = 4\, D_u t\, e^{-2D_u t}, \tag{76}$$

$$\langle[\mathbf{R}_0(t) - \mathbf{R}_0(0)]^2\rangle = 6\, D_r t, \tag{77}$$

$$\langle \mathbf{u}_0(t)\cdot\mathbf{u}_0(0)\rangle = \langle \mathbf{e}_i(t)\cdot\mathbf{e}_i(0)\rangle = e^{-2\, t\, D_u} \tag{78}$$

$$\langle[\mathbf{r}_0(t) - \mathbf{r}_0(0)]^2\rangle = 6\, D_r t, \tag{79}$$

where $i \in \{x, y\}$ and

$$D_u = \frac{3T}{\zeta L^3} \quad , \quad D_r = \frac{T}{\zeta L}. \tag{80}$$

As defined in Eq. (34), the unit vector $\hat{\mathbf{u}}_0(t)$ measures the dynamics of the rigid rod axis while the 2D vector $L^{-1/2}\mathbf{U}_0(t)$ measures the $O(\epsilon)$ deviation of the axis of the semiflexible filament from that of a rigid rod so that

$$\hat{\mathbf{u}}_0^{(1)} = \frac{\hat{\mathbf{u}}_0 + L^{-1/2}\mathbf{U}_0}{|\hat{\mathbf{u}}_0 + L^{-1/2}\mathbf{U}_0|}.$$

Finally from Eq. (35), $\mathbf{r}_0(t)$ measures the dynamics of the center of the rigid rod while the 2D vector $\mathbf{R}_0(t)$ measures the deviation of the motion of the center of mass of the filament from the rigid rod value so that $\mathbf{r}_0^{(1)} = \mathbf{r}_0 + \mathbf{R}_0$. From these equations we can obtain the relevant global timescales of the filament. The rotation time is

$$\tau_{\rm rot} = \frac{1}{2D_u},$$

while the translational diffusion time is

$$\tau_{\rm tran} = \frac{L^2}{2D_r}.$$

IV. RESULTS

With the techniques and to within the approximations of the previous section, we can calculate any dynamic correlation function of the chain. To illustrate the approach, we calculate the dynamics of the mean-square end-to-end distance and the tangent correlation function. For short times we recover the results obtained by expanding about a stationary reference state [6,50,51] and we cross over to a regime dominated by the global modes for longer times.

A. End-to-end fluctuations

The end-to-end distance is defined as $\boldsymbol{\rho}(t) \equiv \mathbf{r}(L,t) - \mathbf{r}(0,t)$ and from the definitions in Eqs. (30), (34), (35), and (49) the mean-square end-to-end distance $\delta\boldsymbol{\rho}^2(t) \equiv \langle[\boldsymbol{\rho}(t) - \boldsymbol{\rho}(0)]^2\rangle$ has a global (G) contribution and a *coupled* or mixed (M) contribution given by

$$\delta\boldsymbol{\rho}^2(t) = \delta\rho_G^2(t) + \delta\rho_M^2(t), \tag{81}$$

where

$$\delta\rho_G^2(t) = [2L^2 + 4L\langle\rho_z(t)\rangle][1 - \langle\hat{\mathbf{u}}_0(t)\cdot\hat{\mathbf{u}}_0(0)\rangle] + L\langle[\mathbf{U}_0(t) - \mathbf{U}_0(0)]^2\rangle, \tag{82}$$

$$\delta\rho_M^2(t) = 2\langle\rho_z^2(t)\rangle - 2\langle\rho_z(t)\rho_z(0)\rangle\langle\hat{\mathbf{u}}_0(t)\cdot\hat{\mathbf{u}}_0(0)\rangle. \tag{83}$$

The component of $\boldsymbol{\rho}(t)$ along the axis $\hat{\mathbf{u}}_0(t)$ is given by $\rho_z(t) = \int_\omega e^{-i\omega t}\rho_z(\omega)$ where $\rho_z(\omega)$ is defined in Eq. (61). Note that $\mathbf{U}_0\cdot\hat{\mathbf{u}}_0 = 0$ by construction. In this expression we see that in addition to the global modes which can be subtracted out that there is a mixed relaxation of internal [given by $\rho_z(t)$] and global rotation modes.

The full expression is rather cumbersome and given in Appendix B. We evaluate numerically and plot in Fig. 5 the mixed part of the end-to-end fluctuation $\delta\rho_M^2(t)$ versus t in units of $\tau_1^{-1} = 2A\pi^4/\zeta L^4$ for various values of $\nu = 2\pi L_p/L$. We used the first 1000 terms in Eq. (B2). We see $t^{3/4}$ scaling at very short times but see deviations at intermediate times before the crossover to the saturation regime.

We can, however, simplify the expression, Eq. (81), in two regimes.

For $t \ll \tau_1$, the correlation function is dominated by the modes with high k and we can replace the sums in Eq. (B2) by integrals. In this regime,

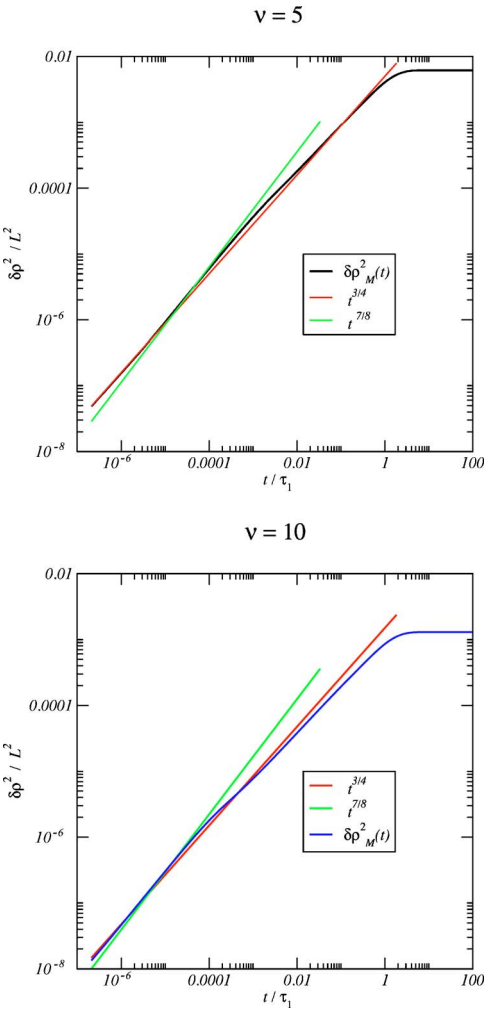

FIG. 5. (Color online) The mixed contributions $\delta\rho_M^2$ to the end-to-end fluctuations in units of τ_1, calculated using the first 1000 modes, showing the mixed scaling at short times. We show $\nu = 5$, 10. The power laws $t^{3/4}$, $t^{7/8}$ are shown as guides to the eye.

$$\langle\delta\boldsymbol{\rho}^2(t)\rangle = \frac{L^2}{\pi^2}\left\{\frac{32\Gamma\left(\frac{1}{4}\right)}{3\nu^2}\left(\frac{t}{\tau_1}\right)^{3/4} + \frac{64\Gamma\left(\frac{1}{8}\right)}{7\pi\nu^{3/2}}\left(\frac{t}{\tau_1}\right)^{7/8}\right\}, \tag{84}$$

where $\nu = 2\pi L_p/L$. The second term in Eq. (84) is always subdominant as can be seen by the following simple argument. At the shortest times, because $t \ll \tau_1$, the $t^{3/4}$ term dominates but one expects that deviations from 3/4 scaling to appear at intermediate times, for $(t/\tau_1)^{1/8} \gg \nu^{-1/2}$, from the $t^{7/8}$ term. The $t^{7/8}$ term comes from the last term on the RHS of Eq. (B2), which we have approximated by an integral for short times. But for $(t/\tau_1)^{1/8} \gg \nu^{-1/2}$, all the modes in this term which decay like $\exp(-k^8\nu^4 t/\tau_1)$ would have relaxed.

For $t > \tau_1$, the correlation function is dominated by the long-lived bending modes and the global motions:

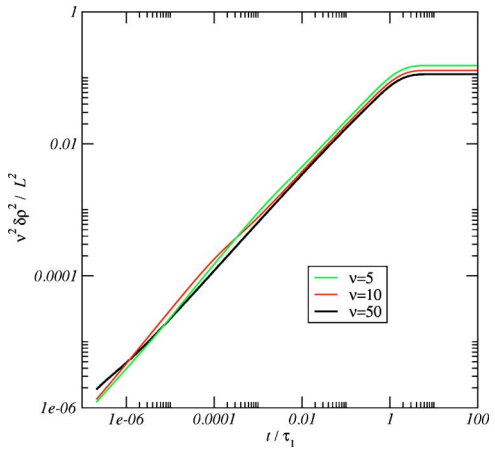

FIG. 6. (Color online) The rescaled correlation function $\nu^2 \delta\rho_M^2/L^2$ for $\nu=5$, 10, 50 calculated using the first 1000 modes.

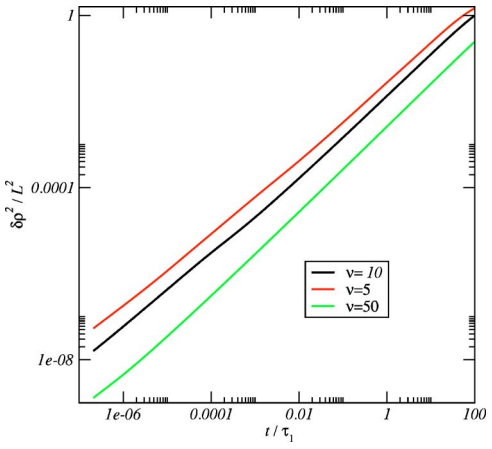

FIG. 7. (Color online) The complete end-to-end fluctuation including all the contributions $\delta\boldsymbol{\rho}^2=\delta\rho_M^2+\delta\rho_G^2$. We included the first 1000 modes.

$$\langle \delta\boldsymbol{\rho}^2(t)\rangle = \left(2L^2 - \frac{4L^3}{L_p}\right)(1-e^{-2D_u t}) + 4L^2 D_u t\, e^{-2D_u t} + \frac{L^2}{\pi^2}\sum_k \frac{32[d(k\nu)-4(k\nu)^2]}{k^2 f(k\nu)} + \frac{2L^4}{9L_p^2} + \frac{L^2}{\pi^2}\sum_k \frac{64}{\pi\nu}\frac{(1-\cos k\pi)}{k^8\nu^4}, \tag{85}$$

where $d(x)$ and $f(x)$ are defined in Appendix B.

Using the analytic result for early times, we rescaled the numerical value of $\delta\rho_M^2(t)$ obtained from the first 1000 terms for different values of ν in Fig. 6. We find a partial collapse on a master curve which is not exact because of the mixing with global rotation modes. Note that rotational relaxational dynamics changes with ν because

$$D_u t = \frac{1}{2\pi^3\nu}\left(\frac{t}{\tau_1}\right).$$

Finally the total function $\delta\boldsymbol{\rho}^2(t)$ given by Eq. (81) is plotted against t in Fig. 7 for different values of ν.

B. Orientational correlations

Another aspect of filament dynamics that can be measured [17] is the orientational dynamics of a tagged section of a semiflexible filament [6]. From Eqs. (29), (34), and (58), we can obtain the orientational correlation of a tagged point on a filament as which also has global and mixed "components":

$$\mathcal{C}(s,t) = \langle[\hat{\mathbf{u}}(s,t)-\hat{\mathbf{u}}(s,0)]^2\rangle = \mathcal{C}_G(s,t) + \mathcal{C}_M(s,t), \tag{86}$$

where

$$\mathcal{C}_G(s,t) = 2[1-\langle\hat{\mathbf{u}}_0(t)\cdot\hat{\mathbf{u}}_0(0)\rangle], \tag{87}$$

$$\mathcal{C}_M(s,t) = \langle[\mathbf{U}(s,t)-\mathbf{U}(s,0)]^2\rangle + \langle|u_z(s,t)|^2\rangle + \langle|u_z(s,0)|^2\rangle - \langle\hat{\mathbf{u}}_0(t)\cdot\hat{\mathbf{u}}_0(0)\rangle\langle u_z(s,t)u_z(s,0)\rangle, \tag{88}$$

where we have taken the limit $\ell/L\to 0$.

The complete expression given in Appendix B for $\mathcal{C}(s,t)$ is rather cumbersome. We can evaluate it numerically for the full range of time scales but we can obtain simple analytic expressions for it in two regimes.

For $t\ll\tau_1$, the correlation function is dominated by the modes with high p and we can replace the sums in Eq. (B4) by integrals and $\phi_p^2(s)=(1/2)(1+\cos 2\hat{p})\simeq 1/2$ far from the ends of the filament. The correlation function is

$$\mathcal{C}(s,t) = \frac{L\Gamma\left(\frac{3}{4}\right)}{L_p\pi^2}\left(\frac{t}{2\tau_1}\right)^{1/4} + \frac{L^2\Gamma\left(\frac{3}{4}\right)}{6L_p^2\pi^2}\left(\frac{t}{\tau_1}\right)^{1/4} \times\left[1-\frac{6\Gamma\left(\frac{3}{4}\right)}{\pi^2}\left(\frac{t}{\tau_1}\right)^{1/4}\right]. \tag{89}$$

The early time $t^{1/4}$ scaling is in agreement with previous work [6,8]. For $t\gg\tau_1$, the correlation function is dominated by the global modes and the correlation function is

$$\mathcal{C}(s,t) = 2(1-e^{-2D_u t}). \tag{90}$$

In Fig. 8, we plot the mixed part of the orientational correlation function given in Eq. (B4) evaluated using the first 1000 modes for the midpoint and endpoints of a filament for various values of ν. We see a crossover from $t^{1/4}$ scaling at early times to the saturated regime at late times. As expected the scaling regime is much cleaner and wider for the midpoint than the endpoints.

The global contribution to the orientational correlation function is plotted in Fig. 9 and the sum of the global and mixed contributions is plotted in Fig. 10 for various values of ν.

V. SUMMARY AND DISCUSSION

We have proposed a way to study the dynamics of an inextensible and semiflexible filament. We have emphasized the fact that such filaments are *constrained* to be both *connected* and *inextensible*. A theoretical treatment of this constrained problem entails starting with either an explicitly connected object that is constrained to be inextensible or an

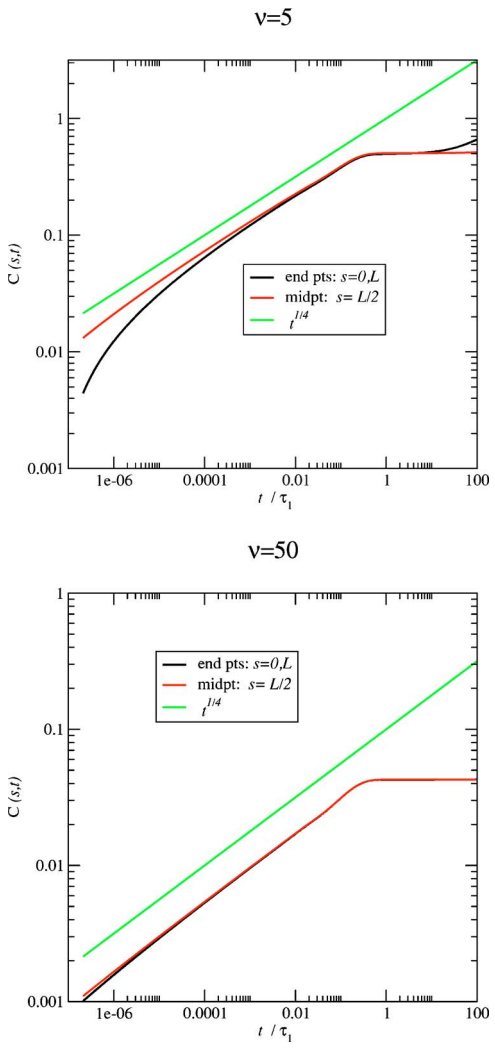

FIG. 8. (Color online) The mixed contributions to $\mathcal{C}(s,t)$ evaluated at the endpoints and the midpoint using the first 1000 modes for $\nu=5$, 50.

explicitly inextensible object which is constrained to be connected.

In contrast to previous approaches which began with explicitly connected chains and imposed the nonlinear constraint of inextensibility on its motion, we began with a filament which by construction is inextensible but whose motion is constrained so as to always *remain* connected. We find that this leads to one extra equation but a *linear* constraint.

To illustrate the new approach, we calculated several dynamic correlation functions of a semiflexible filament of length L which were measured in some recent experiments. Our results are valid for L/L_p small. We recover results obtained earlier for the short-time dynamics of semiflexible fluctuating filaments but are able to capture the crossover of the dynamics from a regime dominated by internal motions of the filament to global translation and rotation.

We find that the global rotation modes always "mix" with internal modes and can only safely ignored for very-short-time behavior. Therefore they should be included in any theory which attempts to capture the dynamical behavior of filaments at intermediate time regimes.

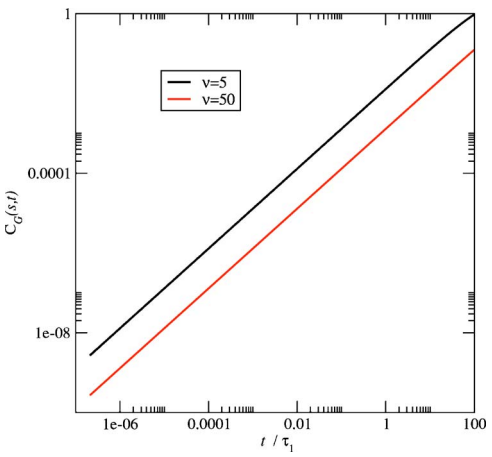

FIG. 9. (Color online) The global contributions to the tangent correlation function evaluated at $\nu=5$, 50.

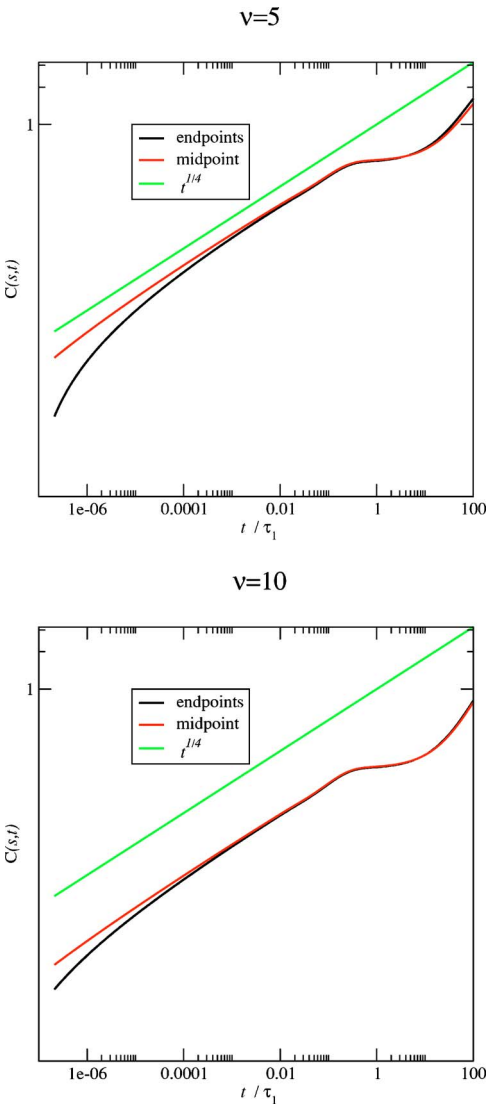

FIG. 10. (Color online) The total tangent correlation function $\mathcal{C}(s,t)$ evaluated at $\nu=5$, 10.

We calculate self-consistently the end-to-end fluctuations of a single filament and find, in agreement with earlier self-consistent calculations (using the traditional approach), a mixed early-time scaling regime with a mixture of the dominant $t^{3/4}$ scaling and the subdominant correction scaling as $t^{7/8}$.

We also obtain the tangent correlations of a tagged point on the filament which could be measured using fluorescence microscopy or coherent neutron scattering. We find in agreement with earlier work [6,51] a $t^{1/4}$ scaling which saturates at a crossover time scale $\tau_1 \sim L^4 \eta / A$.

Using our description, we are also able to determine the relevant time scales for the various global modes of the filament and how they couple to the internal fluctuations.

From our analysis, we are able to observe that the scaling arguments and self-consistent calculations performed earlier correspond to a very reasonable preaveraging approximation similar in spirit to that used for the Zimm model in flexible polymer dynamics.

Finally, this formalism looks like a promising way to study carefully situations such as strongly pushed or pulled filaments interacting with molecular motors [17,22,23].

ACKNOWLEDGMENTS

The author wishes to thank R. Everaers, E. Frey, R. Granek, A. Levine, L. LeGoff, F. MacKintosh, A.C. Maggs, M. Pasquali, D. Morse, V. Shankar, C. Wiggins and the stimulating atmosphere at the KITP for the many helpful discussions which led to this work. Critical comments by O.G. Harlen on a preliminary version of the manuscript are particularly appreciated. This research was supported by the Royal Society.

APPENDIX A: ROTATIONAL BROWNIAN MOTION

Starting from the stochastic dynamics for $\hat{\mathbf{u}}(t)$ in Eq. (1) we can calculate an equation of motion for the probability $P(\hat{\mathbf{n}},t|\hat{\mathbf{n}}_0,0)$ that the rod has orientation $\hat{\mathbf{n}}$ at time t, given it started with orientation $\hat{\mathbf{n}}_0$ at time $t=0$ defined as

$$P(\hat{\mathbf{n}},t|\hat{\mathbf{n}}_0,0) \equiv \langle \delta(\hat{\mathbf{n}} - \hat{\mathbf{u}}(t)) \rangle_{\hat{\mathbf{n}}_0}. \tag{A1}$$

We first note that the form of Eq. (1) makes it clear that changes in $\hat{\mathbf{u}}(t)$ occur via infinitesimal rotations. More explicitly, we can parametrize the proper rotations which belong to the group SO(3) by successive rotations about three mutually orthogonal fixed axes [39]. The rotation matrices are corresponding to rotations about z,x,y or (u_3,u_1,u_2) axes by angles ϕ_3,ϕ_1,ϕ_2 are, respectively,

$$R_3(\phi_3) = \begin{pmatrix} \cos\phi_3 & -\sin\phi_3 & 0 \\ \sin\phi_3 & \cos\phi_3 & 0 \\ 0 & 0 & 1 \end{pmatrix}, \tag{A2}$$

$$R_1(\phi_1) = \begin{pmatrix} 1 & 0 & 0 \\ 0 & \cos\phi_1 & -\sin\phi_1 \\ 0 & \sin\phi_1 & \cos\phi_1 \end{pmatrix}, \tag{A3}$$

$$R_2(\phi_2) = \begin{pmatrix} \cos\phi_2 & 0 & \sin\phi_2 \\ 0 & 1 & 0 \\ -\sin\phi_2 & 0 & \cos\phi_2 \end{pmatrix}, \tag{A4}$$

so that we can define a generic rotation by $R(\phi_i) = R_2(\phi_2)R_1(\phi_1)R_3(\phi_3)$.

The rotation matrices can be expanded in a Taylor series about the identity matrix

$$R_i(\phi_i) = R_i(0) + \phi_i \left.\frac{dR_i}{d\phi_i}\right|_{\phi_i=0} + \frac{1}{2}\phi_i^2 \left.\frac{d^2R_i}{d\phi_i^2}\right|_{\phi_i=0} + \cdots = \exp\left[\phi_i \frac{d}{d\phi_i}\right] R_i(0). \tag{A5}$$

Considering the one-parameter subgroup of rotations about the same axis and using the group composition law for successive rotations, $R_i(\phi_i+\psi_i)=R(\phi_i)R(\psi_i)$, in the Taylor series in Eq. (A5) we obtain

$$\frac{dR_i(\phi_i)}{d\phi_i} = \boldsymbol{\varrho}_i \cdot R_i(\phi_i) \text{ where } \boldsymbol{\varrho}_i = \left.\frac{dR_i}{d\phi_i}\right|_{\phi_i=0}, \tag{A6}$$

defining the matrices $\boldsymbol{\varrho}_i$. From the definition of the rotation matrices, we have

$$\boldsymbol{\varrho}_1 = \begin{pmatrix} 0 & 0 & 0 \\ 0 & 0 & -1 \\ 0 & 1 & 0 \end{pmatrix}, \tag{A7}$$

$$\boldsymbol{\varrho}_2 = \begin{pmatrix} 0 & 0 & 1 \\ 0 & 0 & 0 \\ -1 & 0 & 0 \end{pmatrix}, \tag{A8}$$

$$\boldsymbol{\varrho}_3 = \begin{pmatrix} 0 & -1 & 0 \\ 1 & 0 & 0 \\ 0 & 0 & 0 \end{pmatrix}. \tag{A9}$$

The matrices $\boldsymbol{\varrho}_i$, called the generators of the rotation group, satisfy the commutation relation

$$[\boldsymbol{\varrho}_i, \boldsymbol{\varrho}_j] = \epsilon_{ijk}\boldsymbol{\varrho}_k, \tag{A10}$$

illustrating the fact that rotations do not commute. The higher-order derivatives can be obtained from successive derivations of Eq. (A6)—i.e., $d^nR_i/d\phi_i^n|_{\phi_i=0} = \boldsymbol{\varrho}_i^n$.

Using Eq. (A5), the rotation matrices for any finite angle can be written in terms of the generating matrices $\boldsymbol{\varrho}_i$ in the compact form

$$R_i(\phi_i) = \boldsymbol{\delta} + \phi_i\boldsymbol{\varrho}_i + \frac{1}{2}\phi_i^2\boldsymbol{\varrho}_i^2 + \cdots = \exp(\phi_i\boldsymbol{\varrho}_i). \tag{A11}$$

The generators of the group can be related to differential operators by considering the effect of rotations as coordinate transforms on the arguments of differentiable functions [39]. Infinitesimal rotations (of the unit vector $\hat{\mathbf{u}}$ taking it to $\hat{\mathbf{u}}'$) can be written in terms of the rotation matrices expanded to linear order in the angles ϕ_i:

$$\begin{pmatrix} u_1' \\ u_2' \\ u_3' \end{pmatrix} = \begin{pmatrix} 1 & -\phi_3 & \phi_2 \\ \phi_3 & 1 & -\phi_1 \\ -\phi_2 & \phi_1 & 1 \end{pmatrix} \begin{pmatrix} u_1 \\ u_2 \\ u_3 \end{pmatrix}. \tag{A12}$$

Therefore we observe that the equation of motion for $\hat{\mathbf{u}}(t)$, Eq. (1), gives

$$u_i' = u_i(t+\Delta t) = u_i(t) + \zeta_u^{-1} \int_t^{t+\Delta t} \epsilon_{ijk} u_j(\tau) f_k(\tau) d\tau,$$

corresponding to rotation with angles

$$\phi_i = \zeta_u^{-1} \int_t^{t+\Delta t} f_i(\tau) d\tau \tag{A13}$$

in an infinitesimal time interval Δt.

A function $\Pi(\hat{\mathbf{u}})$ will under an infinitesimal rotation of coordinates become $\Pi(\hat{\mathbf{u}}')$ given by

$$\Pi(u_1', u_2', u_3') = \Pi(u_1 - \phi_3 u_2 + \phi_2 u_3, u_2 + \phi_3 u_1 - \phi_1 u_3, u_3 - \phi_2 u_1 + \phi_1 u_2).$$

Expanding to linear order in the angles ϕ_i we obtain

$$\Pi(u_1', u_2', u_3') = \Pi(u_1, u_2, u_3) + (\phi_1 \mathcal{R}_1 + \phi_2 \mathcal{R}_2 + \phi_3 \mathcal{R}_3) \Pi(u_1, u_2, u_3), \tag{A14}$$

where

$$\mathcal{R}_i = u_j \frac{\partial}{\partial u_k} - u_k \frac{\partial}{\partial u_j} = \epsilon_{ijk} u_j \frac{\partial}{\partial u_k} = \boldsymbol{\varrho}_i \cdot \hat{\mathbf{u}} \cdot \partial_{\hat{\mathbf{u}}}, \quad \vec{\mathcal{R}} = \hat{\mathbf{u}} \times \partial_{\hat{\mathbf{u}}}. \tag{A15}$$

It is straightforward to but cumbersome to extend this relationship to arbitrary order in ϕ_i for $\mathcal{C}^\infty$ functions. For our purposes we need to go to quadratic order in ϕ_i. Given a $\hat{\mathbf{u}}' = R(\phi_i) \cdot \hat{\mathbf{u}} = \Pi_{i=1}^3 \exp[\phi_i \boldsymbol{\varrho}_i] \cdot \hat{\mathbf{u}}$, where here the $\boldsymbol{\varrho}_i$ refer to the matrices defined in Eqs. (A7)–(A9), then there exists the relationship between $\Pi(\hat{\mathbf{u}}')$ and $\Pi(\hat{\mathbf{u}})$ given by

$$\Pi(\hat{\mathbf{u}}') = \Pi(\hat{\mathbf{u}}) + \left(\sum_{i=1}^3 \phi_i \mathcal{R}_i \right) \Pi(\hat{\mathbf{u}}) + \frac{1}{2} \left(\sum_{i,j=1}^3 \phi_i \phi_j \mathcal{R}_i \mathcal{R}_j \right) \Pi(\hat{\mathbf{u}}) + \left(\sum_{i<j}^3 \phi_i \phi_j \boldsymbol{\varrho}_i \cdot \boldsymbol{\varrho}_j \cdot \hat{\mathbf{u}} \cdot \partial_{\hat{\mathbf{u}}} \right) \Pi(\hat{\mathbf{u}}) + O(\phi_i^3), \tag{A16}$$

where the $\mathcal{R}_i$ refer to the differential operators defined in Eq. (A15).

Using Eq. (A16), the probability distribution defined in Eq. (A1), and noting that $\partial_{\hat{\mathbf{n}}} \delta(\hat{\mathbf{n}} - \hat{\mathbf{u}}) = -\partial_{\hat{\mathbf{u}}} \delta(\hat{\mathbf{n}} - \hat{\mathbf{u}})$, we can calculate the probability at time $t + \Delta t$ in terms of the probability at t,

$$P(\hat{\mathbf{n}}, t+\Delta t | \hat{\mathbf{n}}_0, 0) = P(\hat{\mathbf{n}}, t | \hat{\mathbf{n}}_0, 0) + \left(\sum_{i=1}^3 \phi_i \mathcal{R}_i \right) P(\hat{\mathbf{n}}, t | \hat{\mathbf{n}}_0, 0) + \frac{1}{2} \left(\sum_{i,j=1}^3 \phi_i \phi_j \mathcal{R}_i \mathcal{R}_j \right) P + \left(\sum_{i<j}^3 \phi_i \phi_j \boldsymbol{\varrho}_i \cdot \boldsymbol{\varrho}_j \cdot \hat{\mathbf{n}} \cdot \partial_{\hat{\mathbf{n}}} \right) P, \tag{A17}$$

where ϕ_i are defined in Eq. (A13) and $\mathcal{R}_i = \epsilon_{ijk} n_j \partial_{n_k}$.

Using the properties of the averages of the random functions $\mathbf{f}(t)$ given in Eq. (3) we obtain the rotational diffusion equation for P,

$$\partial_t P(\hat{\mathbf{n}}, t | \hat{\mathbf{n}}_0, 0) = D_r \vec{\mathcal{R}}^2 P(\hat{\mathbf{n}}, t | \hat{\mathbf{n}}_0, 0), \tag{A18}$$

where $\vec{\mathcal{R}} = \hat{\mathbf{n}} \times \partial_{\hat{\mathbf{n}}}$ and $\vec{\mathcal{R}}^2 = \Sigma_{i=1}^3 \mathcal{R}_i^2$. It is easy to generalize these arguments to calculate the equation of motion for the probability distribution $P[\{\hat{\mathbf{u}}(s,t)\}]$ for an ensemble of links with orientations $\{\hat{\mathbf{u}}(s,t)\}$ starting from Langevin equations for their dynamics [1].

APPENDIX B: CORRELATION FUNCTIONS

1. End-to-end fluctuations

In this appendix we present the explicit expressions for the end-to-end distance fluctuations defined by Eq. (81), Using Eqs. (76) and (78), the global contribution to the correlation function $\delta\rho_G^2(t)$ is given by

$$\delta\rho_G^2(t) = \left(2L^2 - \frac{4L^3}{L_p} \right) (1 - e^{-2D_u t}) + 4L^2 D_u t \, e^{-2D_u t} + \frac{2L^4}{9L_p^2}. \tag{B1}$$

The mixed contribution to the mean-square end-to-end distance can be expressed using the dimensionless quantity $\nu = 2\pi L_p / L$ relating the length of the filament to the persistence length and the relaxation time of the longest-lived bending mode, $\tau_1 = (\zeta / 2A)(L/\pi)^4$.

From Eq. (61), we obtain

$$\delta\rho_M^2(t) = \frac{L^2}{\pi^2} \sum_k \frac{32[d(k\nu)(1 - e^{-k^4 t/\tau_1 - 2tD_u}) - 4(k\nu)^2 (1 - e^{-2tD_u - k^8 \nu^4 t/\tau_1})]}{k^2 f(k\nu)} + \sum_k \frac{64}{\pi\nu} \frac{(1 - \cos k\pi)[1 - e^{-2tD_u - k^8 \nu^4 t/\tau_1}]}{k^8 \nu^4}, \tag{B2}$$

where

$$d(x) = (x^3 + x^2/\sqrt{2} - 1/\sqrt{2})(x+1)(x^2+1)$$

and

$$f(x) = (x^8 - 1).$$

It is important to note that *all* the dynamic modes relax as $\exp[-2D_u t - Ck^{\phi} t]$— i.e., with a time scale that goes like $\tau_k \sim 1/(Ck^{\phi} + 2D_u)$.

2. Tangent correlations

Here we present the explicit expressions for the correlation functions defined by Eq. (86). Using Eq. (78), the global component is given by

$$\mathcal{C}_G(s,t) = 2(1 - e^{-2D_u t}). \tag{B3}$$

The mixed modes are calculated using Eq. (58) and noting that, from Eq. (33), $u_z(s,t) = -1/2|\mathbf{U}(s,t)|^2$ so that we find

$$\mathcal{C}_M(s,t) = \frac{2L^2}{L_p \pi^2} \sum_{p=1}^{\infty} \frac{1}{p^2} (1 - e^{-p^4 t/2\tau_1 - 2D_u t}) \phi_p^2(s) + \frac{4L^4}{L_p^2 \pi^4} \left(\sum_{p=1}^{\infty} \frac{1}{p^2} \phi_p^2(s) \right)^2 - e^{-2D_u t} \left(\frac{2L^4}{L_p^2 \pi^4} \right) \times \left\{ \left(\sum_{p=1}^{\infty} \frac{1}{p^2} \phi_p^2(s) \right)^2 + \left(\sum_{p=1}^{\infty} \frac{1}{p^2} \phi_p^2(s) e^{-p^4 t/\tau_1} \right)^2 \right\}. \tag{B4}$$

Again it is important to note the mixed relaxation of the modes.

The results above were obtained for $\ell/L \to 0$. We can also obtain the correlation functions of the internal modes for arbitrary ℓ/L— for example,

$$\langle [\mathbf{U}(s,t) - \mathbf{U}(s,0)]^2 \rangle = \sum_{p=1}^{\infty} \phi_p^2(s) \kappa_p^2 \tau_p (1 - e^{-t/\tau_p} \cos \omega_p t), \tag{B5}$$

where $\tau_p^{-1} = (\Delta_p/\kappa_p)\cos(\theta_p/2)$ and $\omega_p = (\Delta_p/\kappa_p)\sin(\theta_p/2)$. The parameters $\Delta_p = A(p\pi/L)^4$ and $\kappa_p^2 = \zeta^2 + \zeta_u^2 (p\pi/L)^4$ while $\sin\theta_p = 2\zeta\zeta_u (p\pi/L)^2/\kappa_p^2$ and $\theta_p \in \{0, \pi\}$. The limit $\ell/L \to 0$ recovers the first term on the RHS of Eq. (B4)

[1] M. Doi and S. F. Edwards, *The Theory of Polymer Dynamics* (Oxford University Press, New York, 1986).
[2] M. Fixman, J. Chem. Phys. **69**, 1527 (1978).
[3] P. Grassia and E. J. Hinch, J. Fluid Mech. **308**, 255 (1996); E. J. Hinch, *ibid.* **74**, 317 (1976); **271**, 219 (1994).
[4] O. Kratky and G. Porod, Recl. Trav. Chim. Pays-Bas **68**, 1106 (1949).
[5] D. C. Morse, Macromolecules **31**, 7030 (1998); **31**, 7044 (1998).
[6] R. Granek, J. Phys. II **7**, 1761 (1997).
[7] F. Gittes and F. MacKintosh, Phys. Rev. E **58**, R1241 (1998).
[8] E. Farge and A. C. Maggs, Macromolecules **26** , 5041 (1993); F. Amblard, A. C. Maggs, B. Yurke, A. N. Pargellis, and S. Leibler, Phys. Rev. Lett. **77**, 4470–4473 (1996).
[9] R. E. Goldstein and S. A. Langer, Phys. Rev. Lett. **75**, 1094 (1995).
[10] U. Seifert, W. Wintz, and P. Nelson, Phys. Rev. Lett. **77**, 5389 (1996).
[11] P. Dimitrakopoulos *et al.*, Phys. Rev. E **64**, 050803(R) (2001).
[12] D. C. Morse, Adv. Chem. Phys. **128**, 65 (2003).
[13] G. B. Whitham, *Linear and Nonlinear Waves* (Wiley, New York, 1974).
[14] R. Everaers F. Jülicher, A. Adjari, and A. C. Maggs, Phys. Rev. Lett. **82**, 3717 (1999).
[15] M. Pasquali, V. Shankar, and D. C. Morse, Phys. Rev. E **64**, 020802(R) (2001); V. Shankar, M. Pasquali, and D. C. Morse, J. Rheol. **46**, 1111 (2002).
[16] T. B. Liverpool and A. C. Maggs, Macromolecules **34**, 6064 (2001).
[17] L. Le Goff, F. Amblard, and E. Furst, Phys. Rev. Lett. **88**, 018101 (2001).
[18] K. Takiguchi, J. Biochem. (Tokyo) **109**, 520 (1991); R. Urrutia *et al.*, Proc. Natl. Acad. Sci. U.S.A. **88**, 6701 (1991).
[19] D. Humphrey, C. Duggan, D. Saha, D. Smith, and J. Käs, Nature (London) **416**, 413 (2002).
[20] F. J. Nédélec, T. Surrey, A. C. Maggs, and S. Leibler, Nature (London) **389**, 305 (1997).
[21] T. Surrey, F. J. Nédélec, S. Leibler, and E. Karsenti, Science **292**, 1167 (2001).
[22] T. B. Liverpool, A. C. Maggs, and A. Ajdari, Phys. Rev. Lett. **86**, 4171 (2001).
[23] T. B. Liverpool, Phys. Rev. E **67**, 031909 (2003).
[24] J. Howard, *Mechanics of Motor Proteins and the Cytoskeleton* (Sinauer, New York, 2000).
[25] G. H. Nyland *et al.*, J. Chem. Phys. **105**, 1198 (1996).
[26] H. C. Öttinger, Phys. Rev. E **50**, 2696 (1994).
[27] M. Doi, J. Polym. Sci., Polym. Phys. Ed. **19**, 229 (1981); N. Kuzuu and M. Doi, J. Phys. Soc. Jpn. **52**, 3486 (1983); M. Doi, Faraday Symp. Chem. Soc. **18**, 49 (1983).
[28] D. Forster, Phys. Rev. Lett. **32**, 1161 (1974); G. Marrucci, Mol. Cryst. Liq. Cryst. Lett. **72**, 153 (1982); A. Semenov, Sov. Phys. JETP **58**, 321 (1983); F. Affouard, M. Kroger, and S. Hess, Phys. Rev. E **54**, 5178 (1996).
[29] S. D. Lee and R. B. Meyer, Phys. Rev. Lett. **61**, 2217 (1988); J. Chem. Phys. **84**, 3443 (1986).
[30] R. Mazo, *Brownian Motion* (Oxford University Press, New York, 2000).
[31] H. Maeda and N. Saito, J. Phys. Soc. Jpn. **27**, 984 (1969).
[32] S. Broersma, J. Chem. Phys. **32**, 1626 (1960).
[33] L. G. Leal and E. J. Hinch, J. Fluid Mech. **46** 685 (1971).

[34] J. M. Rallison and L. G. Leal, J. Chem. Phys. **74**, 4819 (1981).
[35] J. B. Hubbard and P. G. Wolynes, J. Chem. Phys. **69**, 998 (1978).
[36] D. Schaefer *et al.*, J. Chem. Phys. **55**, 3884 (1971).
[37] J. K. G. Dhont, *An Introduction to Dynamics of Colloids* (Elsevier, Amsterdam, 1996).
[38] C. W. Gardiner, *Handbook of Stochastic Methods: For Physics, Chemistry and the Natural Sciences* (Springer-Verlag, New York, 1996).
[39] B. A. Dubrovin, A. T. Fomenko, and S. P. Novikov, *Modern Geometry—Methods and Applications* (Springer-Verlag, New York, 1991).
[40] It transforms like a vector for proper rotations (det=1) but with an opposite sign under improper rotations (det=−1).
[41] Using the fact that the directions of the random forces $\mathbf{f}(t)$ are isotropically distributed, it is straightforward to show that the random forces $\{\mathbf{f}(t)=\mathbf{f}\times\hat{\mathbf{u}}\}$ can be chosen to have the same correlations and distribution as the random torques $\mathbf{f}(t)$.
[42] K. K. Müller-Nedebock, H. L. Frisch, and J. K. Percus, Phys. Rev. E **67**, 011801 (2003).
[43] T. B. Liverpool (unpublished).
[44] Ch. Wiggins *et al.*, Biophys. J. **74**, 1043 (1998).
[45] S. Camalet and F. Jülicher, New J. Phys. **2**, 24.1 (2000).
[46] Like the Rouse model of flexible polymers, this problem requires an *intrinsic* short-distance cutoff for it to be well posed. This cutoff has a physical significance as the length scale below which a continuous description of the polymer (filament) breaks down. This implies a high q (ultraviolet) cutoff Λ in the sums over (Rouse) modes Σ_q^{Λ}. See Chaps. 3 and 4 of Ref. [1]; and Ref. [47].
[47] *Theoretical Challenges in the Dynamics of Complex Fluids*, edited by Tom McLeish (Kluwer, London, 1997).
[48] O. G. Harlen, R. R. Sundararajakumar, and D. L. Koch, J. Fluid Mech. **388**, 355 (1999).
[49] B. Fuchssteiner, Physica D **13**, 387 (1984).
[50] L. Le Goff *et al.*, Phys. Rev. Lett. **89**, 258101 (2002).
[51] K. Kroy and E. Frey, Phys. Rev. E **55**, 3092 (1997).
[52] S. R. Aragorn and S. R. Pecora, Macromolecules **18**, 1868 (1985).